

- 334, 499 (1988); J. W. Putney, Jr., *Cell Calcium* 11, 611 (1990); G. St J. Bird *et al.*, *Nature* 352, 162 (1991)]. Attempts to deplete the  $\text{Ca}^{2+}$  stores with two blockers of the microsomal  $\text{Ca}^{2+}$  adenosine triphosphatase, thapsigargin [Y. Kijima, E. Ogunbunmi, S. Fleischer, *J. Biol. Chem.* 266, 22912 (1991); O. Thastrup, P. J. Cullen, B. K. Drobak, M. R. Hanley, *Proc. Natl. Acad. Sci. U.S.A.* 87, 2466 (1990)] and 2,5-di-(*tert*-butyl)-1,4-benzohydroquinone [G. A. Moore, D. J. McConkey, G. E. N. Kass, P. J. O'Brien, S. Orrenius, *FEBS Lett.* 224, 331 (1987)], applied at extracellular concentrations of 20  $\mu\text{M}$  for 10 min were unsuccessful ( $n = 10$ ). Hydrophobic, membrane-permeant drugs are probably absorbed by the lipophilic yolk platelets [J. N. Dumont, *J. Morphol.* 136, 153 (1972); W. M. Bement and D. G. Capco, *J. Electron Microsc. Tech.* 16, 202 (1990)]. Therefore, it remains uncertain whether depletion of the  $\text{IP}_3$ -sensitive  $\text{Ca}^{2+}$  store itself is a sufficient trigger for  $\text{Ca}^{2+}$  influx in *Xenopus* oocytes.
15. S. DeLisle, K. H. Krause, G. Denning, B. V. L. Potter, M. J. Welsh, *J. Biol. Chem.* 265, 11726 (1990).  $\text{IP}_3\text{S}_3$  has high affinity for the  $\text{IP}_3\text{R}$  of the cerebellum ( $K_d = 31 \pm 3 \text{ nM}$ ) and a median effective concentration ( $\text{EC}_{50}$ ) for  $\text{Ca}^{2+}$  release of  $\sim 5 \mu\text{M}$  in permeabilized Swiss 3T3 cells. In *Xenopus* oocytes,  $\text{IP}_3$  was five to ten times more potent than  $\text{IP}_3\text{S}_3$  in generating oscillations in  $I_{\text{Cl, Ca}}$ . Heparin antagonized both the  $\text{IP}_3\text{S}_3$ -induced waves and the binding of  $\text{IP}_3$  to oocyte microsomes [the amount required for 50% inhibition ( $\text{IC}_{50}$ ) = 2  $\mu\text{g/ml}$ ] (6–9, 13) [B. V. L. Potter, R. A. J. Challis, S. R. Nahorski, *Du Pont Biotech. Update* 5, 1 (1990); C. W. Taylor, M. J. Berridge, K. D. Brown, A. M. Cooke, B. V. L. Potter, *Biochem. Biophys. Res. Commun.* 150, 626 (1988); J. E. Ferguson, B. Potter, R. Nuccitelli, *ibid.* 172, 229 (1990)].
16. Inositol 1,4,5-triphosphate, inositol 2,4,5-triphosphate, and inositol 1,3,4-triphosphate have been shown to induce  $\text{Ca}^{2+}$  influx in *Xenopus* oocytes. In these experiments, the  $\text{Mn}^{2+}$  block of  $I_{\text{Cl, Ca}}$  was used to assay changes in cytosolic  $\text{Ca}^{2+}$  [S. DeLisle, D. Pittet, B. V. L. Potter, P. D. Lew, M. J. Welsh, *Am. J. Physiol.* 262, C1456 (1992); P. M. Snyder, K. H. Krause, M. J. Welsh, *J. Biol. Chem.* 263, 11048 (1988)].
17. Manganese has been used as an indicator of  $\text{Ca}^{2+}$  influx because it quenches indol-1 and fura-2 (Molecular Probes, Eugene, OR) fluorescence [G. Grynkiewicz, M. Poenie, R. Tsien, *J. Biol. Chem.* 260, 3440 (1985)]. We found in some cases that extracellular  $\text{Mn}^{2+}$  (1 to 10 mM) irreversibly increased the Calcium Green signal in  $\text{IP}_3\text{S}_3$ -stimulated oocytes, which suggests that  $\text{Mn}^{2+}$  enhances Calcium Green fluorescence and that the influx pathway is at least partially permeable to  $\text{Mn}^{2+}$ . This makes it unsuitable as an influx channel antagonist in simultaneous imaging and electrophysiological experiments. Conversely, 1 mM  $\text{La}^{3+}$  reliably blocked influx in eight of eight oocytes without affecting the ability of the indicator to respond to  $\text{Ca}^{2+}$ . In the absence of extracellular  $\text{Ca}^{2+}$ , the application of  $\text{La}^{3+}$  did not influence the  $\text{Ca}^{2+}$  waves induced by  $\text{IP}_3\text{S}_3$  (5  $\mu\text{M}$ ).
18. I. Parker and I. Ivorra, *Proc. Natl. Acad. Sci. U.S.A.* 87, 260 (1990).
19. J. B. Parys *et al.*, *J. Biol. Chem.* 267, 18776 (1992). A bell-shaped dependence of  $\text{IP}_3$ -mediated  $\text{Ca}^{2+}$  release on free cytosolic  $\text{Ca}^{2+}$  has also been observed in smooth muscle and rat cerebellar microsomes and in  $\text{IP}_3\text{R}$  channels isolated from rat cerebellum and reconstituted into lipid bilayers [M. Iino, *J. Gen. Physiol.* 95, 1103 (1990); E. A. Finch, T. J. Turner, S. M. Goldin, *Science* 252, 443 (1991); I. Bezprozvanny, J. Watras, B. E. Ehrlich, *Nature* 351, 751 (1991)].
20. N. L. Allbritton, T. Meyer, L. Stryer, *Science* 258, 1812 (1992).
21. We observed regenerative  $\text{Ca}^{2+}$  waves for up to 7 min in the absence of extracellular  $\text{Ca}^{2+}$  after injection of  $\text{IP}_3\text{S}_3$  (100  $\mu\text{M}$ ) in 12 of 16 oocytes.
22. Because Calcium Green does not shift its emission or excitation spectrum upon binding  $\text{Ca}^{2+}$ ,

ratio-metric measurement of  $\text{Ca}^{2+}$  was not possible. Previous measurements set the resting  $\text{Ca}^{2+}$  concentration in oocytes at  $\sim 100 \text{ nM}$  (3, 6–9). Comparison of Calcium Green with dextran-bound Calcium Green indicates that, at the concentrations used, the dye is not a significant mobile  $\text{Ca}^{2+}$  buffer and does not alter our observations.

23. We thank M. Berridge for comments on the work, D. Skuldt and J. Amundson for assistance, A.

Lückhoff for programming, the ANALYZE software group (Mayo Foundation), E. Peralta for the m3AChR plasmid, and K. Hedin and L. Stehno-Bittel for critical review of the manuscript. Supported by the NIH, the Whitaker Foundation, Glaxo Inc., and the J. W. Kieckhefer Foundation. D.C. is an Established Investigator of the American Heart Association.

23 October 1992; accepted 26 January 1993

## Force of Single Kinesin Molecules Measured with Optical Tweezers

Scot C. Kuo\* and Michael P. Sheetz

Isometric forces generated by single molecules of the mechanochemical enzyme kinesin were measured with a laser-induced, single-beam optical gradient trap, also known as optical tweezers. For the microspheres used in this study, the optical tweezers was spring-like for a radius of 100 nanometers and had a maximum force region at a radius of  $\sim 150$  nanometers. With the use of biotinylated microtubules and special streptavidin-coated latex microspheres as handles, microtubule translocation by single squid kinesin molecules was reversibly stalled. The stalled microtubules escaped optical trapping forces of  $1.9 \pm 0.4$  piconewtons. The ability to measure force parameters of single macromolecules now allows direct testing of molecular models for contractility.

Biological forces in motile systems, such as those involving ciliary dynein and actomyosin, are usually studied as the sum of contributions from many force-generating units (1). However, the mechanochemical enzyme kinesin can function as an individual molecule. Kinesin that is adsorbed to glass moves microtubules so that they pivot around a single attachment point (2). The concentration dependence of the motility, calculated as an effective Hill coefficient of 1 for kinesin adsorbed to glass cover slips (2) or as a Poisson distribution for kinesin adsorbed to glass beads (3), indicates that one molecule alone can generate force and move microtubules. We have directly measured the force generated by an individual kinesin molecule using the single-beam optical gradient trap, also known as optical tweezers (4).

To characterize the optical trap, we used viscous drag to displace trapped microspheres that were 0.55  $\mu\text{m}$  in diameter. All calibration experiments were performed at least 2  $\mu\text{m}$  from the cover slip surface to minimize viscous coupling to the glass surface, so deviations from Stokes drag were  $< 7\%$  (5). For all biological force measurements, we calibrated the escape force ( $F_{\text{esc}}$ ) from the optical tweezers by using a laminar flow cell (6). However, optical forces during escape from the op-

tical tweezers are spatially complex, requiring nanometer-level characterization of the optical trap to interpret subsequent experiments. Such characterization would be biased by the shear gradient of the flow cell, so we used viscous forces that were generated by moving the microscope specimen with a piezoceramic-driven stage (7). The stage had a maximal usable velocity of  $\sim 150 \mu\text{m s}^{-1}$  ( $\sim 0.8 \text{ pN}$  of viscous drag), making it less appropriate for direct calibration of biological force measurements. Trapped particles were alternately displaced by the piezoceramic stage moving at constant velocity, and their positions were monitored while laser irradiation was reduced (Fig. 1A). Normalized to the laser irradiation at the specimen, a force and displacement profile can be constructed (Fig. 1B). Force is proportional to the displacement for the first  $\sim 100 \text{ nm}$ . This force-displacement profile qualitatively agrees with theoretical models of the optical trap (8). Because of video limitations, the region of maximum force has not been precisely determined, but it appears to be located at a radius of  $150 \pm 26 \text{ nm}$  (SD) (Fig. 1C).

Optical forces were applied to streptavidin-coated latex microspheres that were attached as handles to biotinylated microtubules. The biotinylation procedure, both with and without the attachment of microspheres, did not alter kinesin-driven gliding velocities of the microtubules. After evaluating different procedures for constructing biotin-specific beads (9), we covalently attached bovine serum albumin to carbodiim-

Department of Cell Biology, Duke University Medical Center, Durham, NC 27710.

\*To whom correspondence should be addressed at the Department of Biomedical Engineering, Johns Hopkins University Medical School, Baltimore, MD 21205.

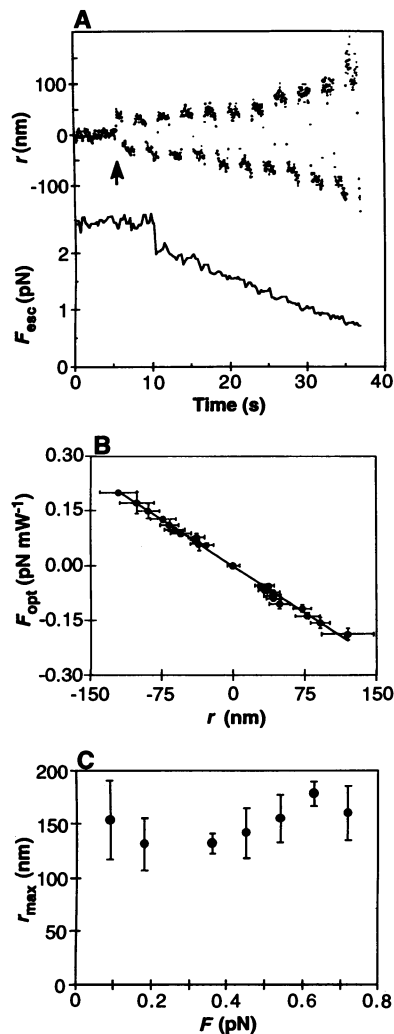


**Fig. 1.** Spatial force profile of the optical tweezers. (A) The position ( $r$ ) of a 0.55- $\mu\text{m}$  microsphere trapped 2  $\mu\text{m}$  above the cover slip was tracked by video as the laser power was simultaneously monitored (15). After the bead was trapped, a triangle-wave voltage displaced the piezoelectric stage at 140  $\mu\text{m s}^{-1}$  in alternating directions ( $t = 5.4$  s, arrow). At  $t = 10$  s, the laser irradiation and corresponding escape force ( $F_{esc}$ ) were reduced by a large step, and smaller reductions were performed at subsequent 1.9-s intervals. (B) Balanced against viscous forces, the optical force was normalized to the laser irradiation at the specimen ( $F_{opt}$ , mean  $\pm$  SD) and was plotted against the displacement of the trapped bead (mean  $\pm$  SD). The root-mean-square deviation of the particle position increased as the laser irradiation was reduced, corresponding to larger thermally induced (Brownian) position fluctuations and a decreased spring constant. The apparent spring constant (stiffness) of the optical tweezers was 1.8 pN  $\mu\text{m}^{-1}$  mW. (C) As the laser irradiation is decreased before particle escape, the maximum excursion ( $r_{max}$ ) of a trapped particle should correspond to the region of maximal force for the optical trap. Over different measurements (mean  $\pm$  SD) at different stage velocities, this maximum force region was located at  $\sim 150 \pm 26$  nm for 0.55- $\mu\text{m}$  microspheres.

ide-activated carboxylate microspheres, followed by limited biotinylation and subsequent binding in saturating amounts of streptavidin. More than 90% of these beads could bind to biotinylated microtubules and remained attached despite forces as great as 10 pN. To increase the association time between kinesin and microtubules, we used subsaturating concentrations of guanosine triphosphate (GTP) as the energy source for kinesin. In our experimental conditions, as many as half of the squid kinesin molecules were active for translocation.

In kinesin force measurements, immobilized kinesin pulls on a biotinylated microtubule that is balanced by optical forces applied to a streptavidin-coated microsphere some distance from the kinesin molecule (Fig. 2C). The position of the trapped microsphere (Fig. 2C) that is determined from video images (Fig. 2B) was monitored while laser power was reduced (Fig. 2C). At  $t = 11.7$  s (Fig. 2C, 1), the microsphere started to move from the center of the optical trap, and its position indicates the balance between mechanical, biological, and optical forces. Because we continuously varied optical forces, a

residual translocation (2.2 nm  $\text{s}^{-1}$ ) was apparent and reduced the quality of stalling kinesin (5% of unloaded velocity). After  $t = 59.4$  s (Fig. 2C, 3), the biological forces exceeded the maximum optical force of the optical tweezers (displacement of 130 nm). However, the bead had not completely escaped the influence of the trap because it still moved more slowly than its unloaded velocity. As the bead progressed out of the remainder of the trap, optical forces pushed it slightly out of focus ("popping") (Fig. 2, B and C, 4) and the stretched bead-microtubule continued to relax; both phenomena appear to shorten the microtubule. Also described for other optical tweezers (10) and their models (8), the popping behavior was seen in all experiments and is beyond the region of maximum force ( $\sim 250$  nm versus  $\sim 150$  nm) (Fig. 1). With the optical tweezers off, the microtubule traveled at unloaded velocity (44 nm  $\text{s}^{-1}$ ) and freely pivoted around its attachment point, which is consistent with movement by a single kinesin molecule.

Because of the limited spatial accuracy of our tracking technique ( $\sim 10$  nm) and

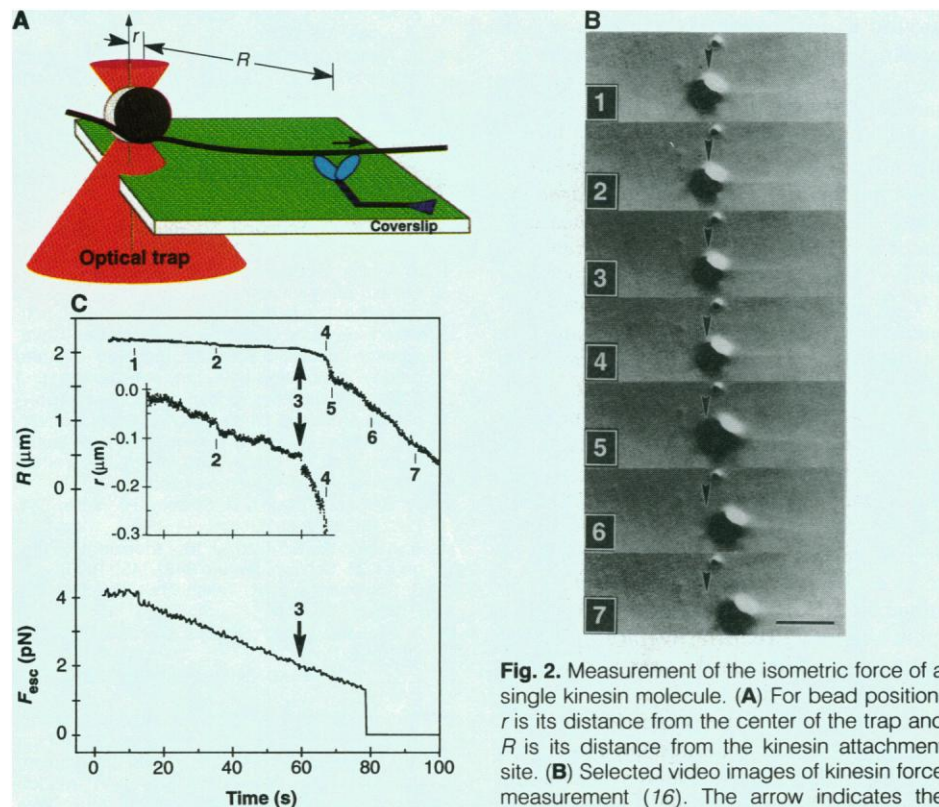


**Fig. 2.** Measurement of the isometric force of a single kinesin molecule. (A) For bead position,  $r$  is its distance from the center of the trap and  $R$  is its distance from the kinesin attachment site. (B) Selected video images of kinesin force measurement (16). The arrow indicates the position of the optical trap, and the particle at the base of the arrow is a 140-nm bead adsorbed to the glass surface as a reference marker. Images 1 to 7 correspond to  $t = 11.7, 35.1, 59.4, 67.1, 69.1, 80.4,$  and  $93.4$  s. Scale bar is 3  $\mu\text{m}$ . (C) Movement of a microtubule-attached bead due to a single kinesin molecule with 1 mM GTP was monitored as the laser power of the optical trap was reduced (16). The bead's position,  $R$  and  $r$  (inset), was calculated from video tracking of the bead's image, as described in Fig. 1. From calibrations of particle escape induced in a flow cell, the bottom trace is the equivalent  $F_{esc}$  of the trap. Numbers 1 to 7 marked along the traces correspond to the elapsed times in (B).

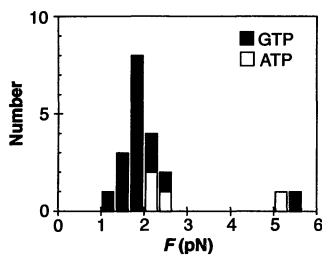


**Fig. 3.** Histogram of kinesin force measurements. Measurements as described in Fig. 2 were repeated with many kinesin molecules. Experiments were performed at nucleotide concentrations of 0.3 to 1 mM GTP (solid bars) or 10  $\mu$ M ATP (open bars). Individual videos were examined for isometric stalling of kinesin (no obvious movement for at least 30 s) and stability of the microscope stage ( $< 1$  nm  $s^{-1}$  of drift when 140-nm reference beads were tracked). The two discrete peaks in the histogram are  $1.9 \pm 0.4$  pN (SD,  $n = 18$ ) and 5.4 pN ( $n = 2$ ).

the compliance of the microtubule-bead tether, the force fluctuations of kinesin are poorly resolved while generating isometric tension. Furthermore, the inherent nanometer-position instabilities of the laser, microscope stage, and video images severely limited our accuracy in measuring the isometric forces using the force-displacement curve (Fig. 1B). Instead, we used the escape force located at  $\sim 150$ -nm radius (Fig. 1C). For the experiment in Fig. 2, kinesin-driven movement escapes at 2.0 pN and corresponds in concept to the isometric tension measured in muscle studies.

This procedure was repeated for many kinesin molecules (Fig. 3). Before and after each valid measurement, the pivoting action of the moving microtubule around a single point was used as a supporting criterion for movement by an individual kinesin molecule. Because of the duration of these measurements, microtubules usually detached from kinesin before it could escape the trap. Both microtubule detachment and drift of the microscope stage disqualified about 90% of measurement attempts. Preliminary measurements with 10  $\mu$ M adenosine triphosphate (ATP) fall within the envelope of GTP measurements (Fig. 3), but the small sample size precludes any distinctions between ATP and GTP. The discrete peak at 5.4 pN ( $n = 2$ ) is consistent with multiple kinesin molecules pulling on the same microtubule, but additional experiments are needed for quantitative interpretation. Finally, the residual translocation velocity ( $\sim 5\%$ ) seen in our motor-stalling protocol reduces the accuracy of our isometric technique by 5 to 10%. Despite this inaccuracy, we estimate that the average isometric force of an individual kinesin molecule is  $1.9 \pm 0.4$  pN (SD).

Our estimate of the isometric force of a single molecule of kinesin compares favorably with other measurements of biological forces. Other experiments with optical tweezers estimated *in vivo* forces of vesicle transport as  $\sim 2.6$  pN per motor molecule (11). A similar attempt with kinesin-coated silica beads was unsuccessful because single motor-coated beads detached from microtubules (3). For sea urchin

sperm flagella, glass microneedle measurements were  $\sim 1$  pN per dynein arm (12). For a muscle fiber, 1 to 2 pN per cross bridge is expected (13), and with stiffness as an estimate of cross bridge number, measurements indicate as much as 2 pN per cross bridge (14). From noise analysis of actomyosin *in vitro*, randomly oriented myosin heads produced 0.4 pN per cross bridge (1). If we assume a similar model for motility, the equivalent number for the two-headed kinesin molecule would be 0.95 pN per cross bridge.

## REFERENCES AND NOTES

1. A. Ishijima, T. Doi, K. Sakurada, T. Yanagida, *Nature* **352**, 301 (1991).
2. J. Howard, A. J. Hudspeth, R. D. Vale, *ibid.* **342**, 154 (1989).
3. S. M. Block, L. S. B. Goldstein, B. J. Schnapp, *ibid.* **348**, 348 (1990).
4. A. Ashkin, J. M. Dziedzic, T. Yamane, *ibid.* **330**, 769 (1987); S. C. Kuo and M. P. Sheetz, *Trends Cell Biol.* **2**, 116 (1992); S. M. Block, *Nature* **360**, 493 (1992).
5. A. J. Goldman, R. G. Cox, H. Brenner, *Chem. Eng. Sci.* **22**, 637 (1967); *ibid.*, p. 653.
6. S. C. Kuo, J. Gelles, E. Steuer, M. P. Sheetz, *J. Cell Sci. Suppl.* **14**, 135 (1991).
7. J. Fu, R. D. Young, T. V. Vorburger, *Rev. Sci. Instrum.* **63**, 2200 (1992).
8. A. Ashkin, *Biophys. J.* **61**, 569 (1992).
9. For 0.5- $\mu$ m microspheres, both direct covalent attachment (water-soluble carbodiimide activation of carboxylate microspheres or Covaspheres from Duke Scientific, Palo Alto, CA) and passive adsorption of avidin, streptavidin, and antibody antibodies (both monoclonal and polyclonal) produced biotin-specific beads that varied greatly in quality. Frequently they would detach from the biotinylated microtubules when piconewton forces were applied.
10. W. Sato, M. Ohyumi, H. Shibata, H. Inaba, *Opt. Lett.* **16**, 282 (1991).
11. A. Ashkin, K. Schütze, J. M. Dziedzic, U. Euteneuer, M. Schliwa, *Nature* **348**, 346 (1990).
12. S. Kamimura and K. Takahashi, *ibid.* **293**, 566 (1981).
13. A. F. Huxley, *Prog. Biophys. Biophys. Chem.* **7**, 255 (1957).
14. \_\_\_\_\_ and R. M. Simmons, *Nature* **233**, 533 (1971).
15. The optical trap used in these experiments was modified from the one described in (6) with the substitution of a Quantronix 116F Nd:yttrium-aluminum-garnet laser (Smithtown, NY). In addition, we modified the piezoelectric stage (Wye Creek, Frederick, MD) with parallel plates containing a water-glycerol mixture to dampen mechanical oscillations. A computer-controlled rotating half-wave plate in a polarization-based attenuator allowed fine control of the laser intensity, and a custom digitizing video overlay (sampling frequency of 4 to 15 Hz) monitored the laser intensity. The viscous force was calculated

from Stokes drag for a sphere ( $F = 6\pi\eta rV$ ), and the stage velocity ( $V$ ) was measured from video images of 0.55- $\mu$ m beads adsorbed to the cover slip surface. Trapped 0.55- $\mu$ m beads were coated in bovine serum albumin (BSA, 1 mg  $ml^{-1}$ ) to prevent adsorption to the glass. The position of the trapped particle was calculated with an intensity-weighted centroid of images recorded on sVHS video tape (6).

16. Motility and force measurements were performed in flow chambers constructed with Dow high-vacuum silicone grease on acid-washed glass cover slips on aluminum holders [B. J. Schnapp, *Methods Enzymol.* **134**, 561 (1986)] that were modified for 22-mm square cover slips. After the adsorption of 140-nm carboxylate microspheres (Polysciences, Warrington, PA) as reference markers, squid kinesin dilutions (typically 0.05 to 1 molecule per square micrometer) were adsorbed for 2 min in the presence of casein (150  $\mu$ g  $ml^{-1}$ ), 100 mM Pipes (pH 6.8), 1 mM  $MgSO_4$ , and 1 mM EGTA. Motility assays were performed at room temperature in the same buffer supplemented with 20  $\mu$ M taxol and nucleotide (GTP or ATP). Force measurements required us to wash the chambers free of unattached biotinylated microtubules and unpolymerized biotinylated tubulin just before introducing streptavidin-coated microspheres. The beads were attached to translocating, biotinylated microtubules with the optical tweezers. This instrument was calibrated after every experimental session by laminar flow (6). The kinesin was purified from *Loligo pealeii* with the use of microtubule affinity as described by R. D. Vale, T. S. Reese, and M. P. Sheetz [*Cell* **42**, 39 (1985)] with the addition of velocity sedimentation through a sucrose gradient [B. J. Schnapp and T. S. Reese, *Proc. Natl. Acad. Sci. U.S.A.* **86**, 1548 (1989)]. With BSA standards, densitometric scanning of Coomassie-stained polyacrylamide gels was used to estimate kinesin concentrations. Heterodimeric tubulin was biotinylated according to the procedure of T. J. Mitchison and M. W. Kirschner [*J. Cell Biol.* **101**, 755 (1985)] and A. Hyman *et al.* [*Methods Enzymol.* **196**, 478 (1991)], mixed 1:1 to 1:8 molar ratios with unmodified tubulin, and polymerized in motility buffer containing 1 mM GTP but lacking casein. We constructed covalent, biotinylated beads coated with BSA at room temperature by activating 0.55- $\mu$ m carboxylate microspheres (Polysciences, Warrington, PA) with 1-(3-dimethylaminopropyl)-3-ethylcarbodiimide (EDC; Aldrich Chemical Co., Milwaukee, WI) [EDC (40 mg  $ml^{-1}$ ) in 100 mM sodium phosphate (pH 4.5) for 30 min] and washing twice by centrifugation in phosphate-buffered saline (PBS) [20 mM phosphate (pH 7.4), 140 mM NaCl, and 10 mM KCl]. The beads were then incubated with BSA (10 mg  $ml^{-1}$ ) in PBS (PBS-BSA) for 30 min, washed twice with PBS, biotinylated with a 30-min incubation with 20 to 100  $\mu$ M NHS-XX-biotin (Molecular Probes) added from a 50 mM stock in dimethyl sulfoxide, quenched with 67 mM glutamate (2 M stock) and BSA (5 mg  $ml^{-1}$ ), washed twice by centrifugation with PBS-BSA, and stored-refrigerated with 0.02% azide. Beads were bath sonicated to break up aggregates formed during centrifugations;  $>95\%$  of the particles are single beads when observed on the microscope. Before they were used, beads were incubated overnight with streptavidin (1 mg  $ml^{-1}$ ) (Sigma) in PBS-BSA, washed three times by centrifugation through a cushion containing 7.5% sucrose in PBS-BSA, and resuspended in PBS-BSA.
17. We thank Y. E. Goldman for comments at a preliminary stage of the work. S.C.K. was a fellow of the Jane Coffin-Childs Memorial Fund for Medical Research. Supported by grants from the National Institutes of Health (GM 36277 and NS 23345) (M.P.S.).

28 October 1992; accepted 21 January 1993